Fracture Mechanics of Concrete Structures, de Borst et al (eds) © 2001 Swets & Zeitlinger, Lisse, ISBN 90 2651 825 0

Mechanical performance of RC and SFRC tunnel lining segments

M.Quiertant, J.F.Seignol & F.Toutlemonde
Laboratoire Central des Ponts et Chaussées, Paris, France

ABSTRACT: An experimental study was carried out to compare mechanical performance of two types of precast tunnel lining segments. First, classical reinforced concrete (RC) segments were loaded up to failure in a configuration corresponding to the critical *in situ* laying loading. Then, full-scale experimental specimens of steel fibre reinforced concrete (SFRC) segments were tested in the same way. In addition to the direct experimental comparison, the study also provides a large data base to refine design methods of classical lining reinforcement and to validate the French design method for SFRC structures acting as beams. In order to ensure a clear analysis of structural behavior of segments, experimental results are analyzed using concurrently a three-dimensional finite elements modeling and an engineering approach providing analytical solutions.

1 INTRODUCTION

The reinforcement cages of precast concrete tunnel lining segments have been generally considered as expensive and labor consuming, due to the specific geometry of the sections. In addition they require an important storage space in the precast factory. However, recent studies have clearly demonstrated the capacity of fibers to be used in the reinforcement of concrete structures (Casanova et al. 1997). From the technical point of view, the benefits of such reinforcing techniques are numerous. For instance, steel fibre reinforced concrete (SFRC) segments are much less subject to impact spalling during *in situ* placement and/or transport.

Consequently, the validity of an alternative solution of SFRC tunnel lining segments was to be tested. Preliminary experimental studies were carried out by Schrub & Ebert (1995) and Toutlemonde et al. (1997). For both types of loading applied during these experimental tests (respectively transverse bending leading to oval-shaping of the lining and pure compressive load applied some cm away from the mid-surface), SFRC segments demonstrated satisfactory performance.

Recently, conventional reinforced concrete (RC) and SFRC segments were tested at LCPC (Laboratoire Central des Ponts et Chaussées) in a configuration considered to be critical for design and corresponding to the *in situ* laying loading. RC elements were thus tested as reference samples. This was regarded as an opportunity to complete and/or validate design methods of the reinforcement of RC tunnel lining segments.

This paper relates briefly this experimental campaign and particularly focuses on the analysis of the test results by different calculation methods. It should be mentioned that deeper numerical analysis, taking into account non-linear behavior (of deformed bars of the reinforcement, damage of concrete...) in the finite element modeling are still in progress. The aim of this paper is thus to draw up a schedule of the current state of the analysis.

2 EXPERIMENTAL STUDY

2.1 *Experimental program*

The experimental program was defined in agreement with AFTES (French association for underground works) recommendations (Guedon 1998) and belongs to a more general study carried out in the frame of the French coordinated R & D program "Projet National BEFIM" (Lacroix & Rossi 2000).

Three segments of each type (RC & SFRC) were used during the experimental campaign.

Material characteristics of segments have been identified on cylinders from the same concrete kept in the same thermal and hygrometric conditions. Moreover, the SFRC characterization in direct tension was made with 36 cylindrical cores drilled from the third SFRC segment (SFR-*c*), following the directions of major extensions as identified during the tests of segments (see Fig. 1).

Three RC companion specimens (RC-*a*, *b* and *c*) and two SFRC (SFR-*a* and *b*) segments were tested. Except RC-*a* (slightly equipped) each sample was equipped with 71 measurement channels (gauges, displacement and load sensors...). This large equipment has permitted to monitor the whole structural behavior of segments, through measurements like vertical and horizontal deflections, as well as the displacements at the axis on inner and outer faces, or local strains along the directions of major compressions (by gauges and by displacement sensors, glued on the surface to capture extensions and crack openings). Main experimental results are available in Toutlemonde et al. (2000b) and are summed up in this paper in a next section concurrently with numerical results.

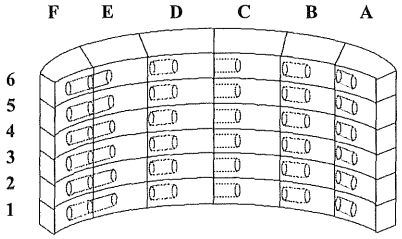

Figure 1. Location of samples cored in the segment SFRC-*c*.

2.2 *Characteristics of tunnel lining segments*

Three SFRC segments and two RC segments were especially cast, in industrial conditions, for the experimental campaign. The third RC segment (referred to as RC-*a* segment), with a shape strictly identical to the other specimens, was also directly coming from a precast factory and was tested during the preliminary test.

All segments are full-scale samples. The ring has an inner diameter of 6.30 m, a thickness of 30 cm, and a length of 1.38 to 1.42 m. The chosen segments have a developed length of 3.96 m (inner side) to 4.34 m (outer side). Details about reinforcement of RC segments and mix-proportions of reference concrete and SFRC are provided in Toutlemonde et al. (2000a).

Mechanical characteristics of the two types of concrete are indicated in Table 1-2. One shall notice a large variation of fiber distribution and measured tensile strength for the 36 of samples cored in the segment SFRC-*c*.

Table 1. Reference concrete and SFRC mechanical characteristics.

	Ref. concrete	SFRC
	At 28 days (water)	
f_c (MPa)	61.0	64.5
f_t (MPa) splitting test	5.0	5.5
	At 11 months (air)	
f_c (MPa)	97.5	74.2
f_t (MPa) splitting test	5.7	
Young's mod. (GPa)	49.7	42.4
Poisson's ratio	0.18	0.18

Table 2. Number of fibers (**n**) and average yield tensile stress (f_t) of samples cored in the segment SFRC-*c* (see also Fig.1) and tested in direct tension.

	A	B	C	D	E	F
1	**86**/2.4	**97**/1.8	**X**	**132**/2.6	**X**	**113**/3.4
2	**X**	**133**/2.2	**86**/2.0	**X**	**57**/0.7	**54**/1.5
n/ft* 3	**53**/0.9	**46**/0.5	**91**/1.8	**48**/0.4	**73**/0.9	**41**/0.9
4	**26**/0.3	**52**/0.5	**102**/2.2	**35**/0.2	**43**/X	**41**/0.4
5	**74**/X	**116**/1.5	**96**/2.0	**45**/0.6	**64**/0.9	**X**/0.7
6	**87**/1.5	**92**/X	**X**	**110**/1.6	**90**/2.5	**110**/2.3

* f_t (MPa) corresponding to a crack opening of 0-0.5 mm
X : no experimental result

2.3 *Experimental frame for testing tunnel segments*

The design of the testing frame is based on a global vertical load capacity of 2.2 MN applied by two annular hydraulic jacks inserted in a closed frame made of struts and ties and fixed to the strong floor of LCPC structures laboratory (Fig. 2).

The supports are as widely apart from the axis as possible (3.16 m is the total span at the mid-surface), to maximize the bending moment.

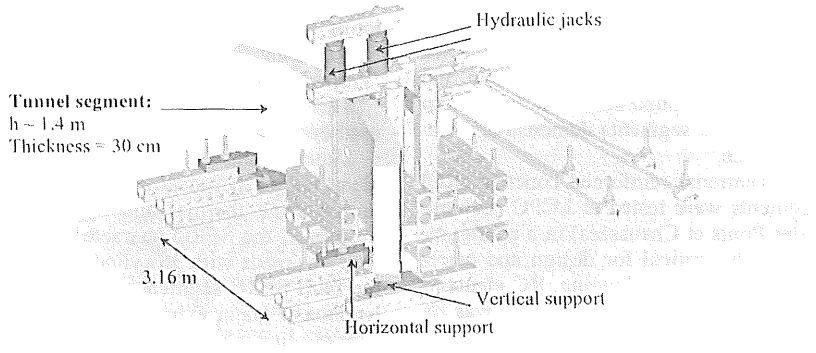

Figure 2. Scheme of the testing frame.

However, since the vertical reactions are not located in the same plane as the applied load, the toppling moment has to be balanced by horizontal support forces. It has been chosen to concentrate the abutments in the vicinity of the zones where vertical loads are applied (see Fig. 3).

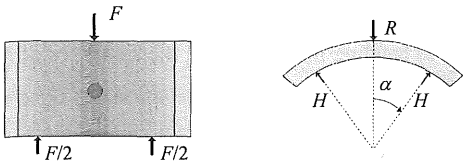

a) Vertical forces b) Horizontal forces

Figure 3. Experimental loading configuration of segments.

In Figure F : Thrust of jacks
$F/2$: Vertical support forces (of lower supports)
R : Upper horizontal support force
H : Lower horizontal support force

3 ANALYTICAL AND NUMERICAL APPROACH

This section presents analytical (Toutlemonde 2000) and numerical methods aimed to analyze the above-mentioned experiments.

Three classical "engineer methods" are briefly described: the classical beam theory allows us to predict the elastic stresses just before concrete cracking; the French BAEL design code is used to evaluate the maximum load of the central section; a simplified struts and tie model represents the segment behavior at ultimate limit state and helps giving a better estimation of the failure load. Eventually, an elastic finite-element simulation is described.

3.1 *Classical beam theory*

This calculation is based on Saint-Venant's hypothesis. The segment is considered as an elastic curved beam. Each section is determined by the angle θ in [-28.5°;28.5°], where θ=0 denotes the central section (see Figure 4). In a particular section, the local coordinates are r in [Ri;Re] (with Ri=3.15 m, Re=3.45 m) and z in [-h/2;h/2] (h=1.42 m).

The loading consists in a vertical force F applied on the top of the central section (r=3.2845 m) balanced by two support forces $F/2$ on the lower rests (at r=3.3 m); the lower horizontal supports produce two radial forces H, which must be equal to 0.173F. We shall note by $\pm\ \alpha$ the angular position of these abutments (α=28.5°).

For this isostatic structure, this helps computing forces and moments applied to the center of gravity in each section.

We obtain (R_m is the mean radius and e is the segment thickness):

- the normal force $N=-H\sin(\theta-\alpha)$; (1)

- the vertical shear $V_z=F/2$; (2)

- the horizontal shear parallel to the radius

$V_r=-H\cos(\theta-\alpha)$; (3)

- the horizontal bending moment

$M_z=H\,R_m\sin(\alpha-\theta)$; (4)

- the vertical bending moment

$M_r=F\sin(\alpha-\theta)[R_m/2+(h/2-e)\cos(\alpha-\theta)]$; (5)

- the moment of torsion

$M_\theta=FR_m/2[\cos(\alpha-\theta)-1]+H(h/2-e)\cos(\alpha-\theta)$. (6)

The normal and shear stresses will then be obtained from the previous expressions.

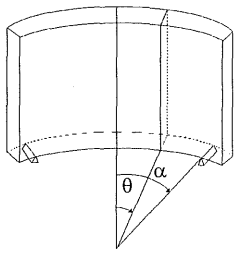

Figure 4. Localization of the current section by the angle θ.

3.1.1 *Critical sections*

From equations (4) and (5), one can conclude that horizontal and vertical bending moments are maximum for θ equal to zero (center of segment). At that location, we obtain M_r= 0,839F, Mz= 0,273F and M_θ=-0,104F *(local maximum)*.

The bending moments cancel for θ equal to α.

A null value of the moment of torsion is obtained with θ equal to 8.2° in equation (6).

3.1.2 *Normal stresses*

Normal stresses result from the combination of the normal tensile force and both vertical and horizontal bending moments. These moments and force all vary as sin(α-θ), hence the neutral axis remains constant in every section. Let us denote by positive values the tensile stresses.

Within the hypotheses of beam theory, we get, for a point (r,z) in any section:

$\sigma(r,z)=N/(bh)+M_r\cdot r/I_r-M_z\,z/I_z$ (7)

where I_r and I_z denote respectively the horizontal and vertical moments of inertia.

3.1.3 *Shear stress*

Stresses produced by horizontal and vertical shear are assumed to be distributed according to parabolic laws, respectively along the r and z axis (as in classical beam theory). The moment of torsion induces stresses constant on curves homothetic to the section border, null at the center, growing with the square of the co-ordinates.

The extreme values for each part of the shear stress are located at mid-height of the faces, for torsion the extreme values are obtained thanks tabulated values corresponding to a ratio of approximately 4 which exists between the width and the height of the section. Main results are :

-The vertical shear stress (due to shear force, directed upwards) is constant and maximum in the mid height of the vertical faces. Its value is $3F/4bh$.

-The horizontal shear stress (due to shear force, directed towards the outer side) is maximum along the average radius and is equal to $3H\cos(\alpha-\theta)/2bh$.

-The shear stress due to torsion is

- a vertical shear stress directed upwards, equal to $2.89F$ in the middle height of the inner side and to $-3.03F$ on supports (opposite values in the middle height of the outer side),
- a horizontal shear stress directed towards the outer side. This shear stress is equal, along the average radius, to $2.15F$ in lowest part, to $-2.25F$ in the center and on supports.

Particular values of combined shear stress are given in section 4.1 (Table 3).

3.2 *Calculation based on BAEL rules*

The French design code BAEL ("Béton armé aux états limites") may be used to evaluate the failure load of the RC segments. These rules are based on the following assumptions:

- concrete in tension is neglected;
- compressed concrete follows the "rectangular-parabolic" constitutive law;
- steel bars are elastoplastic;
- the failure is caused by both horizontal and vertical bending moments, which is equivalent to applying a bending moment in a plan tilted of 7.8°;
- moment of torsion is neglected.

An iterative computation is used to find the position of the neutral axis (see Figure 5).

If we now assume that:

- the central section is critical;
- all inner side horizontal rebars and the five lowest rebars of the outer side are stressed up to the plastic yield (550 MPa);
- the most stressed rebar (located in the bottom of the inner side) has a conventional maximum strain of 10‰;
- the compressive yield stress of the concrete is 95 MPa;

it is then possible to calculate the equilibrium of the section in the center of gravity. This leads to:

- a vertical bending moment of 783 kN.m;
- a horizontal bending moment of 197 kN.m;
- a bending moment along the axis tilted of 7.8° of 300 kN.m.

These different results are not compatible with a single value of the effort in the center of the section. This is discussed in section 4.2.2.

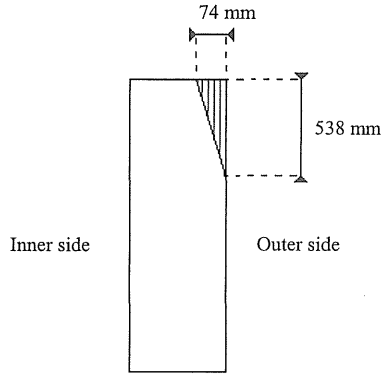

Figure 5 Compressive zone in the central section (BAEL computation).

3.3 *Prediction of the structural failure using struts and tie analysis*

Based on experimental observation, one shall assume that the main mechanism describing behavior of the segment before failure consists in two connecting struts transmitting the vertical load F to the lower supports, and horizontal curved tie joining these two supports, as can be seen on Figure 6. On this figure, β denotes the vertical angle between the struts and the tie, while γ is the horizontal angle. Simple trigonometric rules give β=42° and γ=24.4°.

The above-described outer forces are responsible for the following vertical and horizontal efforts:

$$F_{cv} = F/(2\sin\beta) \quad (8)$$

$$F_{tv} = F_{cv}\cos\beta \quad (9)$$

$$F_{ch} = H\cos\alpha / \sin\gamma \quad (10)$$

$$F_{th} = F_{ch}\cos\gamma + H\sin\alpha \quad (11)$$

Finally, the tie has to resist to $F_t = F_{tv} + F_{th}$.

These results are based on the assumption that the curved tie push is balanced by the reinforcement of the nearby concrete (whichever it consists in fibers or steel bars).

The strength of the tie depends on the type of segment. For RC segments, according to experimental considerations, the resistance is due to the inner-map steel bars as well as the six lowest outer-map bars. These bars are supposed to have a maximal stress of 550 MPa, which yields a total strength of 1119 kN.

For SFRC segments, it is reasonable to consider that the strength is located in the part of the segment under tension, which means in the lower third of the section. Since the SFRC is supposed to have a tensile strength equal to 3.6 MPa, we obtain a total strength of 511 kN for the tie.

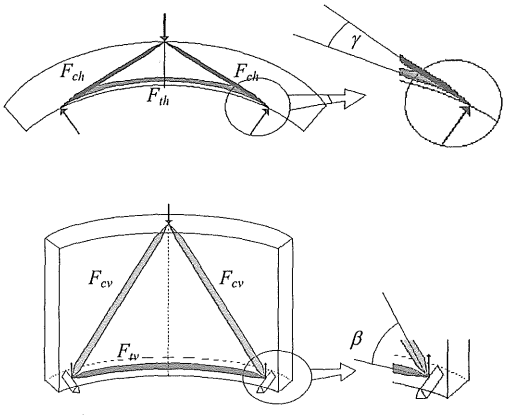

Figure 6. Horizontal and vertical efforts in the struts and tie analysis.

3.4 *Finite elements method*

A first FEM-analysis has been conducted, in order to predict the cracking load. During this state, the concrete is considered as a linear elastic material and the reinforcement is neglected. The elastic parameters are E=42,000 MPa and ν=0.18, which corresponds to the SFRC concrete.

Since the problem is symmetric, half of the segment is modeled by a 3-dimensional mesh, composed of 2,574 8-node hexaedric elements. The mesh, represented on Figure 7, has 9,660 degrees of freedom. The variable size of the different elements is chosen in order to superpose bar elements representing reinforcement steel bars in the case of RC segments.

The hatched squares show the boundary conditions. The dark one is the application zone of the hydraulic jacks. The light ones represent the displacement conditions. Each one is similar to the plate of steel put between the concrete segment and the different abutments. The motion is prevented in the direction normal to the plate. In addition, the orthoradial motion is null on the whole symmetry plane, on the right of the figure.

The first results of this simulation are presented in the next section.

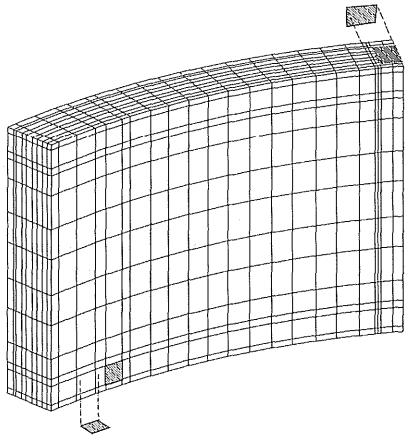

Figure 7. 3D FEM model.

4 COMPARISON BETWEEN EXPERIMENTS AND PREDICTIONS

4.1 *Crack initiation*

The experimental loads corresponding to the crack initiation are summarized in Table 4. We will study in this section the prediction of thess loads by the different methods previously presented.

The equation (7) shows that the normal stress is maximum in the bottom of the inner side. In the same way we have specified that the value of vertical shear is maximum at mid height of the vertical faces, whereas the horizontal shear stress is maximum along the average radius. Normal and shear stress at 7 characteristic locations of the cross-section are considered (see Figure 8 and Table 3).

The point A of the central section corresponds to the *a priori* zone of cracks initiation. By comparing the calculated value (in Table 3) with the tensile strength (by splitting test) of the reference concrete, on shall conclude to a crack initiation for a loading of 234 kN, which is a prediction consistent with experimental results (see Table 6).

For RC segments, after the first cracking, if we assume that the maximum tensile zone spreads over about 50 cm from the axis (which corresponds to the section characterized by θ=8.2°), the tensile strength is reached for a loading of 322 kN. Cracks were ob-

served in that location for a load of (approximately) for a load of 300 kN for SFRC segments.

One shall notice that the initiation of cracks was experimentally observed for RC segments along the inner side vertical reinforcement steel bars, on both sides of the central part of the segment (corresponding to the section defined by θ=8.2°).

In the same way, one can calculate that the tensile strength is reached in the point *D* of the central section for a total load of 385 kN. For cracks in that location, the experimental value of the loading is 400-450 kN for SFRC segments, and is quite higher for RC segments due to the initiation of cracks along the inner side vertical reinforcement steel bars .

For the SFRC segments, we make the hypothesis that cracks appear as soon as a maximum tensile stress of 5.5 MPa is reached, which occurs in the central section for a load equal to 230 kN (see Table 3).

By the FEM modeling, the initiation of cracks can be predicted assuming a tensile strength of 5 MPa for the reference concrete. The corresponding loading is 260 kN. For such a loading, the value of the normal stress in different points of the central section is presented in Table 5 and compared with the elastic prediction calculated from classical beam theory.

Assuming 5.5 MPa of tensile strength for SFRC concrete leads to predict a loading of 286 kN for the crack initiation by the FEM.

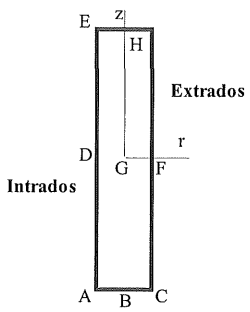

Figure 8. Characteristic points in a current section .

Table 3. Elastic stress in some specific points and sections (from classical beam theory).

	θ=0°		θ=8.2°		θ=28.5°	
	σ	τ	σ	τ	σ	τ
A	21.14*F*	0	15.37*F*	0	0	0
B	8.32*F*	-2.69*F*	6.05*F*	-0.57*F*	0	1.68*F*
C	-4.50*F*	0	-3.27*F*	0	0	0
D	12.82*F*	-1.13*F*	9.32*F*	1.76*F*	0	4.78*F*
E	4.50*F*	0	3.27*F*	0	0	0
F	-12.82*F*	4.65*F*	-9.32*F*	1.76*F*	0	-1.26*F*
H	-8.32*F*	1.61*F*	6.05*F*	-0.57*F*	0	-2.82*F*

Table 4. Experimental load at first crack of the different segments.

Specimen reference	Load (kN)
RC-*a* (prelim.)	200 - 250
RC-*b*	210
RC-*c*	270
SFRC-*a*	300
SFRC-b	300

Table 5. Elastic prediction of the normal stress (MPa).

	FEM	Classical beam theory
A	5.0	4.1
C	-1.0	-0.4
D	3.0	2.0
E	1.1	-1.6

4.2 *Failure*

4.2.1 *Elastic prediction of the stress*

In this section, we use the results of the elastic prediction of normal and shear stress presented in Table 3. However, since cracks are initiated, an elastic prediction must be carefully used, and results must be just considered as an indication.

Bearing capacities of the different segments are presented in Table 6. Typical failures of RC and SFRC segment are shown on Figure 9 and 10.

Table 6. Bearing capacities of the different segments.

Specimen reference	Shear failure load	Maximum load
RC-*a* (prelim.)	870 kN	1170 kN
RC-*b*	900 kN	1140 kN
RC-*c*	900 kN	1130 kN
SFRC-*a*	480 kN	490 kN
SFRC-b	480 kN	490 kN

4.2.1.1 RC segments

However, if we consider that tensile stresses are supported by rebars and if we assume that combined effects of tensile and shear stress are neglected, the ultimate shear stress of concrete is certainly reached at 5 MPa. Then the concrete shear failure will appear for a loading of 1046 kN in support zone (point *D* in section defined by $\theta=\alpha$) and a loading of 1075 kN in point *F* of the central section. This second failure mechanism corresponds to a shear failure due to the torsion.

During the tests, diagonal cracks were noticed at 870-900 kN (see Table 6). This value corresponds to a shear stress of 4 MPa.

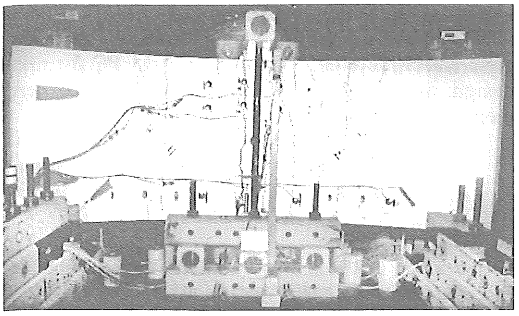

Figure 9: Typical failure of an RC segment (inner face).

4.2.1.2 SFRC segments

Considering SFRC segments, a value of 2 MPa of the tensile stress is reached at the upper part of the inner side of the central section, for an applied loading of 445 kN. If we assume this value of 2 MPa to be equal to the post-peak tensile strength, this result is consistent with the observed failure mode of SFRC segments that occurs for a loading of 490 kN (see Figure 10).

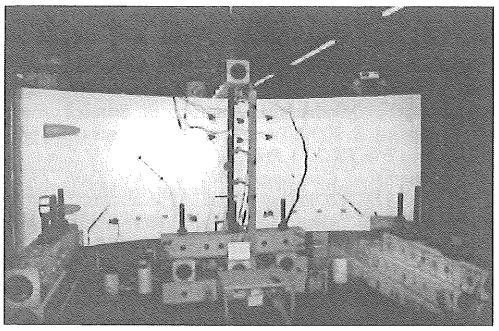

Figure 10: Typical failure of an SFRC segment (inner face).

4.2.2 *Failure prediction based on the French design code BAEL*

From the analysis provided in section 3.2, we have concluded that the different expressions of the bending moment are not valid with a single value of the effort. The resulting values of the effort are 721 kN, 933 kN and 780 kN according to whether one considers respectively the horizontal bending moment, the vertical bending moment or the bending moment along the axis tilted of 7.8°.

In addition, it was checked that another value of the yield stress of steel rebars (600 MPa instead of 550 MPa) did not induce a significant change of the failure load (740 kN instead of the initial value of 721 kN if we consider horizontal bending moment).

Finally, this kind of calculation leads to a pessimistic prediction of the failure load. Particularly, it underestimates the compressive strength of the concrete under transverse restraint at the top of the central section.

Moreover, the examination of failed sample have shown that steel bars of the outer side and at the upper part of the inner side were not so stressed as it was assumed for this calculation (striction or failure of steel bars was observed only in the six lowest bars of the inner side).

We can thus conclude that the central section behavior of segments cannot be directly derived from a classical approach based on the beam theory, even if we include the bi-directional bending in a simplified analysis. Such approach must be particularly perfectible for structure with relatively short span. Moreover, similarly to the deep beams analysis, the hypothesis of plane section must be re-considered.

4.2.3 *Bending - shear interaction for SFRC segments.*

If we assume that:

- the ultimate crack opening is 1 mm for a considered lever arm of 1m corresponding to 2/3 of the height of segment (1‰ of equivalent strain);
- the post-peak tensile strength is 2/3 of the maximum tensile stress as long as crack openings are small;
- the post-peak tensile behavior of the SFRC concrete can be modeled by an elastic perfectly-plastic law;

it is then possible to define an ultimate state, where the maximum crack opening is reached at the point *A* of the central section, and where the neutral axis moved towards the outer side. The neutral axis is still supposed to be tilted of 7.8°, thus it passes through the point *C* of the central section.

The calculation of this ultimate limit state leads to total force of 895 kN in the compressive zone, that must be equilibrated by concrete in tension. The resulting moment (calculated in the location of the initial neutral axis) is equal to 168 kN.m. From expressions of moment presented in section 3.1, we deduce a value of the applied load *F* of 438 kN. This is a rather satisfactory result compared to the experimental failure load of 490 kN (see Table 6).

However, it must be emphasized that the value of the tensile strength decreases with the crack opening.

4.2.4 *Struts and tie analysis.*

Equations of the section 3.3 are used to evaluate the failure load. We assume that the tensile strength of the central section only depends of inner side horizontal rebars. Moreover, on ultimate state, the six lowest outer side rebars are supposed to be in tension, thus their tensile strength is tacking into account. The load capacity of the tie is then equal to 1119 kN. This corresponds to *F* equal 1149 kN (for

an average experimental loading of approximately 1150 kN, see Table 6).

For SFRC segments, the strength comes from the tensile zone that is supposed to be equal to the third of the central section. For a tensile strength of 3.6 MPa, this leads to a tie capacity of 511 kN. The corresponding value of the load failure (F) is 525 kN.

5 CONCLUSIONS

Classical RC tunnel segments were tested in comparison with alternative SFRC precast segments, in a critical configuration. The specific structural behavior of both types of segments was precisely identified and checked by numerous sensors.

In addition to this experimental study, a large effort of modeling was conducted to establish an efficient analysis by different calculation methods. These methods are presented and evaluated by comparison of their prediction to experimental results.

For presented analytic methods, hypotheses are not always valid (plane section, elastic behavior ...).

It should be emphasized that deeper non-linear numerical analysis are still in progress. The aim of this work is finally to establish (and validate) design methods either for RC or SFRC tunnel segments.

Moreover, some recent results of the SFRC characterization in direct tension are presented. Unfortunately, these results are too recent to be included in the presented calculations. Nevertheless, they clearly show that the lack of homogeneity in fiber distribution, related to the casting process, has induced considerable variations in the tensile properties of the material. Fibers were thus unable to control crack propagation and post-cracking behavior in the entire structure. This has lead to a premature unstable propagation of a major crack and to a brittle structural behavior. It must be underlined that taking into account an average mechanical characteristic of SFRC leads to neglect the critical zone of low tensile strength which are preponderant in the structural behavior.

6 ACKNOWLEDGEMENTS

This research was supported as part of the national R&D program BEFIM (chaired by R Lacroix and conducted by P. Rossi) devoted to SFRC and sponsored by the French Ministry of Transport and joint efforts of industrial partners, among which Bonna, CB SGE and the LCPC. It is also useful to mention the help of AFTES (French association for underground works) recommendations and of colleagues who made the experiments possible: Mr Pallot (Bonna) and Mr Cortinovis (Bekaert) for segments fabrication, Mr Bascoulergue and Mr Hurez (CB SGE) for computations, F. Atassi (ENTPE) for the SFRC characterization, the Concrete and Structures Departments of LCPC for mix-design, material tests and preparation of the experiments and measurements on segments.

7 REFERENCES

Casanova, P., Rossi, P. & Schaller, I. 1997. Can steel fibers replace transverse reinforcements in reinforced concrete beams. *ACI Materials Journal* 94(5): 341-354.

Guedon, P. 1998. La conception, le dimensionnement et l'exécution des revêtements en voussoirs préfabriqués en béton armé installés à l'arrière d'un tunnelier. *Tunnels et Ouvrages Souterrains* 147: 153-187.

Lacroix, R. & Rossi, P. 2000. BEFIM: The French National Project for the industrial development of metal fibre reinforced concrete. In *PRO 15 Proc. of the 5th RILEM Symp. on Fibre-Reinforced Concretes - BEFIB' 2000, Lyon, 13-15 sept. 2000*: 171-180. France : RILEM Publication.

Schrub & Ebert, 1995. Durchführung von Versuchen an Tübbings mit Stabstahl- und Stahlfaserbewehrung, Research report N°1319/Eb, ref. 3192-11, TU München.

Toutlemonde, F. 2000. Analyse des résultats des essais de voussoirs de tunnel par des méthodes de dimensionnement approchées, BEFIM research report, LCPC, Paris.

Toutlemonde, F., Quiertant, M. & Dubroca, S. 2000. Justification du renforcement des voussoirs préfabriqués des tunnels : Expérimentations sur voussoirs en béton armé et béton de fibres. *Tunnels et Ouvrages Souterrains* 162: 333-341.

Toutlemonde, F., Quiertant, M., Dubroca, S., Rossi, P., Petit, F., & Bernard, S. 2000. Tunnel precast segments : an SFRC alternative ? In *PRO 15 Proc. of the 5th RILEM Symp. on Fibre-Reinforced Concretes - BEFIB' 2000, Lyon, 13-15 sept. 2000*: 171-180. France : RILEM Publication.

Toutlemonde, F., Schaller, I. & Rossi, P. 1997. Expérimentation à l'échelle 1 de voussoirs de tunnel préfabriqués en béton armé et béton de fibres, BEFIM research report, LCPC, Paris.